FUKUSHIMA MEDICAL UNIVERSITY

Title	Tau positron emission tomography in patients with cognitive impairment and suspected Alzheimer's disease
Author(s)	Matsuda, Hiroshi; Yamao, Tensho
Citation	Fukushima Journal of Medical Science. 69(2): 85-93
Issue Date	2023
URL	http://ir.fmu.ac.jp/dspace/handle/123456789/2155
Rights	© 2023 The Fukushima Society of Medical Science. This article is licensed under a Creative Commons [Attribution-NonCommercial-ShareAlike 4.0 International] license.
DOI	10.5387/fms.2023-08
Text Version	publisher

Fukushima Medical University

[Review]

Tau positron emission tomography in patients with cognitive impairment and suspected Alzheimer's disease

Hiroshi Matsuda[1] and Tensho Yamao[2]

[1]*Department of Biofunctional Imaging, Fukushima Medical University*, [2]*Department of Radiological Sciences, School of Health Sciences, Fukushima Medical University*

Abstract

Alzheimer's disease (AD) is diagnosed by the presence of both amyloid β and tau proteins.   Recent advances in molecular PET imaging have made it possible to assess the accumulation of these proteins in the living brain.   PET ligands have been developed that bind to 3R/4R tau in AD, but not to 3R tau or 4R tau alone.   Of the first-generation PET ligands, ^{18}F-flortaucipir has recently been approved by the Food and Drug Administration.   Several second-generation PET probes with less off-target binding have been developed and are being applied clinically.   Visual interpretation of tau PET should be based on neuropathological neurofibrillary tangle staging instead of a simple positive or negative classification.   Four visual read classifications have been proposed : "no uptake," "medial temporal lobe (MTL) only," "MTL AND," and "outside MTL."   As an adjunct to visual interpretation, quantitative analysis has been proposed using MRI-based native space FreeSurfer parcellations.   The standardized uptake value ratio of the target area is measured using the cerebellar gray matter as a reference region.   In the near future, the Centiloid scale of tau PET is expected to be used as a harmonized value for standardizing each analytical method or PET ligand used, similar to amyloid PET.

Key words : Alzheimer's disease, PET, tau, amyloid

Introduction

Alzheimer's disease (AD) has long been considered a clinicopathological entity characterized by a typical amnestic syndrome and the presence of three hallmark pathological features in the postmortem brain : amyloid β plaques, neurofibrillary tangles (NFT), and neurodegeneration[1].   However, it has since been recognized that some patients presenting with a typical clinical syndrome do not have neuropathological amyloidopathy and/or tauopathy[2,3].   Furthermore, patients with neuropathological changes associated with AD at postmortem may clinically present with non-amnestic syndromes[4].   Therefore, various scientific communities, including the National Institute on Aging and Alzheimer's Association, have proposed a biological definition of AD.   This collaboration has jointly released the AD research framework, which defines AD as a function of the presence of biomarkers of amyloidopathy (A), tauopathy (T), and neurodegeneration/neuronal injury (N)[5], as well as the clinical syndrome.   Under this new framework, AD is diagnosed when both A and T are positive, regardless of whether N is positive or negative.

Recent advancements have made it possible to perform in vivo A/T/N classification using cerebrospinal fluid biomarkers and neuroimaging techniques.   Neuroimaging modalities such as amyloid positron emission tomography (PET), tau PET, MRI and/or fluorodeoxyglucose-PET are used to identify the presence of A, T, and N, respectively.   Over the past few years, numerous tracers for amyloid PET have been developed, and standardized methods for

their PET reading and quantification have been established[6]. Additionally, numerous clinical efficacy studies for amyloid PET have been published[7-9]. Similarly, many tau PET tracers have been developed, and their clinical usefulness is being confirmed[10,11]. Accurate A/T/N classification is expected to be of great help in the development of curative treatments for Alzheimer's disease (AD) in the future. Therefore, it is necessary to eliminate the possibility of contamination of these profiles, especially A and T.

Tau is a neuronal microtubule-associated protein that promotes microtubule self-assembly by tubulin and modulates the stability of axonal microtubules. The adult human brain contains six main isoforms of tau, generated by alternative splicing of exons 2, 3, and 10. These isoforms are further categorized by the presence of three or four carboxy-terminal repeat domains, referred to as 3R or 4R tau isoforms, respectively[12]. Depending on the major tau isoforms found in aggregates, tauopathies are classified into 3R tauopathies (primarily containing 3R tau) with a phenotype of Pick's disease, 4R tauopathies (primarily containing 4R tau) with phenotypes of progressive supranuclear palsy, corticobasal degeneration, and argyrophilic grain disease, and 3R/4R tauopathies (with an approximately equal ratio of 3R tau and 4R tau) with phenotypes of AD, primary age-related tauopathy, and chronic traumatic encephalopathy[13]. In this context, tau PET tracers for AD diagnosis should specifically bind to 3R/4R tau isoforms and not to 3R or 4R tau alone. This review article outlines the current status of tau PET tracer development, as well as its reading method and quantitative evaluation.

Clinical significance and research implications

Tau PET ligands
First-generation :

The radioligand 2-(1-{6-[(2-[Fluorine-18]fluoroethyl)(methyl)amino]-2-naphthyl}-ethylidene) malononitrile (^{18}F-FDDNP) is the first PET tracer to visualize AD pathology in living humans[14]. ^{18}F-FDDNP binds to both NFTs and amyloid plaques in the brain. In the first longitudinal PET study comparing tracer binding of ^{11}C-PiB and ^{18}F-FDDNP in AD patients, MCI patients, and healthy controls, ^{18}F-FDDNP successfully discriminated AD from healthy controls with a 9-fold lower specific binding signal, possibly due to both amyloid and tau, compared to ^{11}C-PiB. Interestingly, the development of ^{18}F-FDDNP has opened the door to PET imaging of not only amyloid but also tau in other tau diseases. This is because postmortem histopathological studies have consistently demonstrated that NFT is a better indicator of disease severity and progression than Aβ.

One of the earliest agents developed for tau imaging was ^{11}C-labeled PBB3, a pyrinated phenyl- and pyridinyl-butadienyl-benzothiazole with a 50-fold higher affinity for tau than Aβ deposits[15]. ^{11}C-PBB3 is a PET tracer used clinically for in vivo detection of tau inclusions in AD as well as non-AD tauopathies in the human brain. However, its high white matter uptake, low target-to-white matter ratio in autoradiography of AD tissue, rapid in vivo metabolism, photoisomerization upon fluorescent light exposure, and brain-penetrating metabolites that make ligand uptake difficult to quantify have hindered its utility[16]. It also exhibits high retention in the dural venous sinus. Finally, the short half-life of ^{11}C labeling limits the availability of PET ligands compared to ^{18}F labeling.

Tohoku University has developed a series of quinolone derivatives, including ^{18}F-THK5117[17] and ^{18}F-THK5351[18]. Of the two, ^{18}F-THK5351 has good imaging properties and is characterized by high uptake into gray matter, low uptake into white matter, and low lipophilicity. It shows high affinity for the tau protein isoform with four repeats in the microtubule-binding domain (4R-tau). However, high off-target binding of ^{18}F-THK5351 was observed, especially in the thalamus, where blocking studies with the monoamine oxidase (MAO) B inhibitor selegiline showed a 40% drastic decrease in ^{18}F-THK5351 uptake[19]. Cortical uptake was also significantly reduced due to this off-target binding, indicating that ^{18}F-THK5351 cannot accurately quantify human tau levels in vivo.

The radioligand 7-(6-[^{18}F]fluoropyridine-3-yl)-5H-pyrido[4,3-b]indol, also known as ^{18}F-flortaucipir, ^{18}F-AV1451, or ^{18}F-T807, is the most extensively studied first-generation tau PET tracer[20]. In 2020, it was approved by the U.S. Food and Drug Administration as Tauvid™ for PET imaging of adult patients with cognitive impairments undergoing evaluation for Alzheimer's disease (AD) based on tau pathology[21,22]. The radioligand has high affinity for 3R/4R tau isoforms in AD patients. Autoradiography studies using human brain tissue samples from multiple neurodegenerative disorders have confirmed that ^{18}F-flortaucipir binds specifically to paired helical filaments, tau-containing NFTs, and

dystrophic neurites in AD brains[20,23]. However, there is little or no binding of ^{18}F-flortaucipir to tau aggregates composed of straight filaments, as well as to alpha-synuclein or TDP-43 deposits. Off-target binding is observed in the choroid plexus[24,25]. This finding is of particular interest, as the choroid plexus is a critical area in the study of AD tauopathy, given its proximity to the hippocampus and its potential involvement in a critical stage of AD tauopathy progression. The choroid plexus is a dense collection of capillaries in an ependymal stroma surrounded by a layer of epithelium. Several substances found in the choroid plexus could potentially bind to ^{18}F-flortaucipir, including melanin, which is supported by the fact that Black/African American individuals show higher tracer accumulation in the choroid plexus than White American individuals[26]. Other phenomena found in the choroid plexus that may accumulate ^{18}F-flortaucipir include calcification/mineralization[24], Biondi rings[27], and iron deposits[28]. On the other hand, tangle-like structures of the epithelial cells in the choroid plexus that can be labeled with ^{18}F-flortaucipir may also immunoreact to tau-specific antibodies[29]. This off-target binding should be interpreted with caution, as it primarily affects the measurement of ^{18}F-flortaucipir accumulation in the hippocampus.

MAOs have been identified as a potential source of off-target binding in ^{18}F-flortaucipir PET imaging. Vermeiren et al.[30] reported that ^{3}H-AV1451 binds with high affinity to either MAO-A or MAO-B, depending on the region of the brain being examined. Specifically, the binding of ^{3}H-AV1451 in the temporal cortex is sensitive to clorgyline but not selegiline, indicating that most binding is to MAO-A. Conversely, in the thalamus and subthalamic nucleus, ^{3}H-AV1451 binds equally to selegiline and clorgyline and to MAO-B, consistent with the known relative distribution and abundance of these two enzymes in the human brain. Although ^{3}H-AV1451 has about 10-fold lower affinity for MAO-B than for MAO-A, the levels of MAO-B in the human brain are 2- to 10-fold higher than those of MAO-A, offsetting the lower affinity for MAO-B. However, in a study by Hansen et al.[31], there were no significant differences in ^{18}F-flortaucipir uptake between Parkinson's disease patients who received MAO-B inhibitors and those who did not. This suggests that the use of MAO-B inhibitors at pharmaceutical levels does not significantly affect ^{18}F-flortaucipir binding, and that MAO-B is not a significant binding target for ^{18}F-flortaucipir in clinical studies.

Second-generation :

The second-generation tau PET ligands appear to have overcome several limitations associated with MAO off-target binding, which were observed in first-generation ligands[32]. For instance, ^{18}F-RO948 exhibits low lipophilicity and a relatively low plasma-free fraction. Autoradiographic studies show that it binds with high affinity to tau aggregated in AD brain sections, while exhibiting lower reactivity in non-AD tauopathies. This suggests that ^{18}F-RO948 primarily recognizes a mixture of 3R and 4R tau isoforms[33]. Unlike ^{18}F-flortaucipir, ^{18}F-RO-948 has excellent kinetic properties and appears to be free of off-target retention in the basal ganglia, thalamus, and choroid plexus[34]. Additionally, it lacks affinity for MAO-A and -B. However, Kuwabara et al.[35] reported that off-target ^{18}F-RO948 retention was observed in the substantia nigra and the cerebellar vermis in two young control individuals, which could be attributed to its binding to neuromelanin deposits.

Similarly, ^{18}F-GTP1 exhibits high affinity and selectivity for tau pathology with no measurable binding to Aβ plaques or MAO-B in AD tissues or binding to other tested proteins at an affinity predicted to impede image data interpretation. In humans, it exhibits favorable dosimetry and brain kinetics, and no evidence of defluorination. Moreover, ^{18}F-GTP1-specific binding is observed in cortical regions of the brain predicted to contain tau pathology in AD, and exhibits low test-retest variability[36,37].

^{18}F-PI2620 is structurally similar to ^{18}F-flortaucipir, suggesting similar binding preferences to 3R/4R tau. Specific binding to pathologically misfolded tau was demonstrated by autoradiography on AD brain sections, whereas no specific tracer binding was detected on brain slices from non-demented donors. In addition to its high-affinity binding to tau aggregates, the compound showed excellent selectivity with no off-target binding to Aβ or MAO-A/B[38]. Elevated tau PET signal using ^{18}F-PI2620 was observed in the medial temporal lobe and posterior cortical association areas in typical Aβ+ amnestic MCI and AD dementia[39].

The [^{18}F]-JNJ-64326067-AAA (^{18}F-JNJ067) has high binding to tau and low binding to Aβ. AD participants showed elevated tracer relative to controls in the entorhinal cortex[40]. However, off-target signal in the putamen, pallidum, thalamus, midbrain, superior cerebellar gray, and white matter was observed. Lack of binding in HCs, MCIs, and PSPs suggests that ^{18}F-JNJ067 may not bind to low levels

of AD-related tau or 4R tau.

^{18}F-PM-PBB3, APN-1607, also known as ^{18}F-florzolotau, is a propylated analogue of ^{11}C-PBB3. It was proposed to circumvent the off-target binding of ^{11}C-PBB3, metabolic instability, and the brief half-life of ^{11}C compared with ^{18}F. Unlike ^{11}C-PBB3, there was no sign of off-target binding in the basal ganglia and thalamus, while there was no sign of binding to MAO. PM-PBB3 had more distinct binding in the choroid plexus[41,42]. PM-PBB3 can recognize tau pathologies in both AD and non-AD brains, including progressive supranuclear palsy[41], corticobasal degeneration[43], and Pick's disease[44]. Autoradiography studies of frontal AD brain homogenates showed that ^{18}F-PM-PBB3 has a high binding potential to tau without binding to MAO enzymes and little to Aβ in vitro[41]. However, other in vitro studies[45] demonstrated significant relationships of APN-1607 with amyloid plaque pathology. Co-incubation of ALS patient frontal cortex and motor cortex tissues with ^{3}H-APN-1607 and 10μM amyloid-specific agent NAV-4694 was carried out to define the contribution of Aβ to the radioligand signal and revealed an average inhibition of 25.0±20.4% gray matter. Additionally, off-target binding to α-synuclein fibrils by the parent molecule, ^{11}C-PBB3, and derivatives has been described[46,47]. These studies suggest that APN-1607, the parent compound ^{11}C-PBB3, and derivatives may display binding to a number of pathological proteins.

The radioligand, 6-[^{18}F]fluoro-3-(1H-pyrrolo[2,3-c] yridine-1-yl) isoquinolin-5-amine (^{18}F-MK6240)[48] exhibited low binding to MAO-B in molecular docking studies[49]. Nonhuman primate blocking studies also showed no apparent off-target binding[50]. Several studies have established that the binding patterns of this ligand are associated with NFT deposition in AD[51-53]. Conversely, ^{18}F-MK-6240 does not bind to the entorhinal cortex of the non-AD brain[50]. The tracer displays favorable kinetics with rapid brain delivery and washout without labeling of the white matter[48,50]. The cerebellar gray matter has low binding across individuals, demonstrating its potential use as a reference region. A reversible two-tissue compartment model well described the time-activity curves across individuals and brain regions. Initial ^{18}F-MK6240 PET studies revealed distribution volume values above 4 in the AD cortex, indicating high affinity to NFTs in vivo, accompanied by a low non-displaceable signal[52]. Off-target binding regions included the retina, ethmoid sinus, clivus, meninges, and substantia nigra, but not the basal ganglia or choroid plexus[54].

These off-target bindings are related to melanin and neuromelanin-containing cells[55]. The standardized uptake value ratio (SUVR) of ^{18}F-MK6240 was two to four in NFT-rich regions of AD patients 60-90 minutes after tracer injection, indicating high uptake, while the SUVR was around one throughout healthy control brains[53]. Across all subjects, the tracer exhibited adequate test-retest variabilities for various endpoints in NFT-rich brain areas[56]. The binding pattern of ^{18}F-MK6240 in target areas of amyloid-positive patients without dementia and AD patients correlated with Braak staging [57,58] of NFT accumulation[52,54]. A direct comparative study[59] with ^{18}F-flortaucipir demonstrated complete concordance of visual ratings between the two radiotracers for both the medial temporal lobe and the neocortex, while the dynamic range of SUVR in target regions was approximately two-fold higher for ^{18}F-MK6240 than for ^{18}F-flortaucipir. This greater dynamic range for ^{18}F-MK6240, with much less off-target binding than for ^{18}F-flortaucipir, may be an advantage in detecting early tau pathology or in performing longitudinal studies to detect small interval changes.

Visual interpretation of tau PET

For visual interpretation of tau PET, second-generation tracers with less off-target binding are preferable compared to amyloid PET. This is because amyloid PET may have difficulty detecting mild accumulation in the targeted cortex due to non-specific diffuse white matter accumulation. Visual interpretation of tau PET can be improved by using neuropathological NFT staging instead of a simple positive or negative classification. According to Braak staging, tau propagation can be classified into six stages based on the location of the tangle-bearing neurons and the severity of changes[57,58]. The first two stages, characterized by preferential involvement of the transentorhinal region and mild hippocampal involvement, are known as the "transentorhinal stages." The next two stages, marked by significant involvement of both the entorhinal and transentorhinal regions, mild to moderate hippocampal involvement, and low neocortical involvement, are called the "limbic stages." The final two stages, characterized by devastating neocortical involvement, are known as the "neocortical stages." Pascoal *et al.*[54] suggested using ^{18}F-MK6240 Braak stages based on this neuropathological NFT staging. This staging method can help stratify individuals with abnormal tau deposition in clinical and research settings. An ^{18}F-MK6240 Braak stage of 0

indicates a low risk of amyloid-β pathology, neurodegeneration, and forthcoming cognitive impairment. An ^{18}F-MK6240 Braak stage of IV or above indicates a high risk of underlying neurodegeneration, and an ^{18}F-MK6240 Braak stage of V-VI is associated with impending onset of dementia.

On the other hand, Shuping *et al.*[60] proposed four visual read classifications for ^{18}F-MK6240 : "no uptake," "MTL only," "MTL AND," and "outside MTL." "No uptake" is defined as a lack of elevated ^{18}F-MK-6240 signal in medial temporal or neocortical regions, or signal in any "off-target" brain region such as the striatum, cerebellum, or midbrain that does not exceed the signal in the retina. "MTL only," corresponding to ^{18}F-MK6240 Braak stages I-II, is defined as elevated intensity in any MTL structure, including the transentorhinal, entorhinal, subiculum, hippocampus, parahippocampus, and amygdala, in either hemisphere, without any neocortical uptake. "MTL only" identifies this uptake while distinguishing it from neocortical spread associated with amyloid-dependent disease progression[61,62]. This MTL only accumulation is also observed in primary age-related tauopathy[63,64]. The sagittal slice of PET in AD shows a "hook-like" uptake of strong accumulation in the amygdala and entorhinal area to the parahippocampus and weak accumulation in the hippocampus[65] (Fig. 1a). "MTL AND," corresponding to ^{18}F-MK6240 Braak stages III and above, indicates elevated signal in MTL and at least one additional neocortical region, in either/both hemispheres. Uptake in the lateral temporal neocortex, including anterolateral tissue and fusiform, in frontal, parietal, occipital, and/or cingulate regions all contribute to "AND." "MTL AND" captures neocortical NFT spread associated with AD progression and an accelerated rate of NFT accumulation, the slowing of which is the goal of several clinical trials. This spatial discrimination is relevant to monitoring disease progression and treatment response. "Outside MTL" is defined as uptake in neocortical regions or in subcortical regions other than MTL that exceed retinal intensity. Some scans show focal uptake only in areas with a clinical phenotype different from typical AD, such as the occipital and frontal areas, and cases that show a medial temporal preservation pattern with neocortical uptake typical of AD. Non-brain off-target signal, such as meninges, does not constitute positive uptake.

Quantitative analysis of tau PET

As an adjunct to visual interpretation, quantitative analysis of tau PET has been proposed. However, the significance of quantitative analysis of tau PET in the brain is still in the research stage, and its clinical significance remains to be determined. Establishing a quantitative measurement would contribute to a more objective and longitudinal evaluation, as well as determination of the therapeutic effects of AD-modifying drugs currently under development.

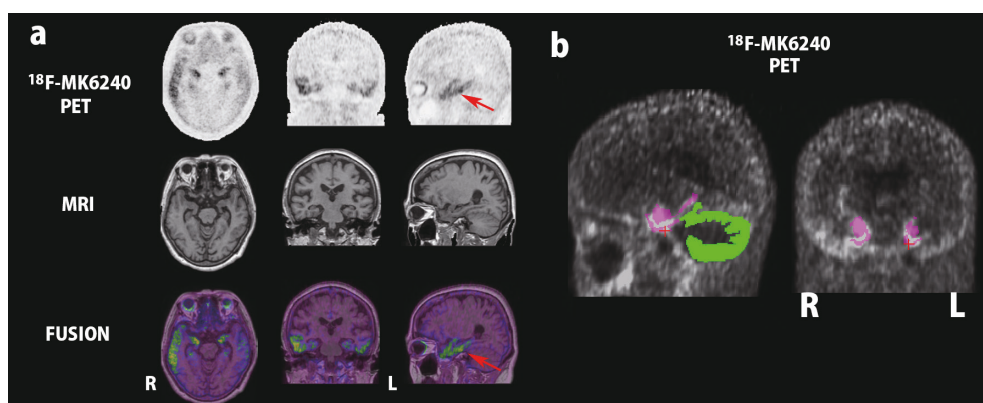Villemagne *et al.*[66] constructed three regional tau masks : mesial-temporal (Me), which comprises

Fig. 1　Tau PET using ^{18}F-MK6240 in a woman with AD in her early 70s
The present study was approved by the certified Clinical Research Review Board at the National Institutes for Quantum Science and Technology, and all subjects or their legal representatives gave written informed consent. This study was registered in the Japan Registry of Clinical Trials (jRCTs 031210318).
a. Visual interpretation with classification of "MTL AND" at Braak stage IV.
Tau accumulation in MTL showed "hook-like" pattern in sagittal sections of PET and FUSION images (arrows).
b. SUVR measures using FreeSurfer parcellation.
Right and left mesial temporal masks (pink) showed SUVRs of 2.21 and 1.69, respectively with a reference mask of entire cerebellar gray matter (green).

the entorhinal cortex, hippocampus, parahippocampus, and amygdala ; temporoparietal (Te), which comprises the inferior and middle temporal, fusiform, supramarginal, and angular gyri, orbitofrontal cortex, gyrus rectus, posterior cingulate/precuneus, superior and inferior parietal, and lateral occipital ; and the rest of the neocortex (R), which comprises the dorsolateral and ventrolateral prefrontal, superior temporal, and anterior cingulate. A global measure of neocortical tau was calculated from the average of the Te and R composite regions.

These tau masks are usually sampled from 3D T1-weighted MRI images that are coregistered to tau PET using MRI-based native space FreeSurfer parcellations[67] (Fig. 1b). Studies have also reported using the inferior cerebellar gray matter as a reference region instead of the entire cerebellar gray matter to avoid contamination from the adjacent cerebellar tentorium and to more accurately estimate standardized uptake value ratio (SUVR)[52,67]. Furthermore, the Centiloid scale is expected to be used as a harmonized value for standardizing each analytical method or PET ligand used, as in amyloid PET[68].

Conclusion

Currently, tau PET is a novel imaging tool for diagnosing patients with cognitive impairment and has great potential in identifying tau pathology in vivo, as well as biologically staging neurodegenerative diseases. Additionally, it aids in distinguishing between AD and other dementia subtypes with overlapping clinical phenotypes, as well as identifying atypical Alzheimer's disease variants. Similar to other molecular neuroimaging biomarkers, such as amyloid PET, the development of tau radiopharmaceuticals shows great promise in advancing the development of disease-modifying therapies for AD and in tauopathy diagnosis. The Aducanumab trial demonstrated that the "amyloid hypothesis" might be true in some patients. In a phase II trial of Donanemab in early symptomatic AD patients with PET evidence of tau and amyloid deposition, amyloid plaque levels and global tau load at week 76 reduced by 85.06 Centiloid and 0.01 greater, respectively, with Donanemab than with placebo[69]. While global tau load was not significantly reduced with Donanemab, greater reductions were observed in frontal and temporal lobe regions. These findings indicate that targeting amyloid-β reduction might prevent cognitive decline by slowing the accumulation of tau in these regions. To achieve the same goal, tau PET has been used as an essential secondary end-point in AD prevention trials with Lecanemab[70].

Conflict of interest disclosure

References

1. Jack CR Jr, Bennett DA, Blennow K, *et al.* Toward a biological definition of Alzheimer's disease. Alzheimers Dement, **14** : 535-562, 2018.

2. Nelson PT, Head E, Schmitt FA, *et al.* Alzheimer's disease is not "brain aging" : neuropathological, genetic, and epidemiological human studies. Acta Neuropathol, **121** : 571-587, 2011.

3. Serrano-Pozo A, Qian J, Monsell SE, *et al.* Mild to moderate Alzheimer dementia with insufficient neuropathological changes. Ann Neurol, **75** : 597-601, 2014.

4. Nelson PT, Alafuzoff I, Bigio EH, *et al.* Correlation of Alzheimer disease neuropathologic changes with cognitive status : a review of the literature. J Neuropathol Exp Neurol, **71** : 362-381, 2012.

5. Jack CR Jr, Bennett DA, Blennow K, *et al.* A/T/N : An unbiased descriptive classification scheme for Alzheimer disease biomarkers. Neurology, **87** : 539-547, 2016.

6. Matsuda H, Shigemoto Y, Sato N. Neuroimaging of Alzheimer's disease : focus on amyloid and tau PET. Jpn J Radiol, **37** : 735-749, 2019.

7. Rabinovici GD, Gatsonis C, Apgar C, *et al.* Association of amyloid positron emission tomography with subsequent change in clinical management among Medicare beneficiaries with mild cognitive impairment or dementia. JAMA, **321** : 1286-1294, 2019.

8. Matsuda H, Ito K, Ishii K, *et al.* Quantitative evaluation of ^{18}F-Flutemetamol PET in patients with cognitive impairment and suspected Alzheimer's disease : a multicenter study. Front Neurol, **11** : 578753, 2021.

9. Matsuda H, Okita K, Motoi Y, *et al.* Clinical impact of amyloid PET using ^{18}F-florbetapir in patients with cognitive impairment and suspected Alzheimer's disease : a multicenter study. Ann Nucl Med, **36** : 1039-1049, 2022

10. Beyer L, Brendel M. Imaging of tau pathology in

neurodegenerative diseases : an update. Semin Nucl Med, **51** : 253-263, 2021.

11. Cassinelli Petersen G, Roytman M, Chiang GC, Li Y, Gordon ML, Franceschi AM. Overview of tau PET molecular imaging. Curr Opin Neurol, **35** : 230-239, 2022.

12. Wang Y, Mandelkow E. Tau in physiology and pathology. Nat Rev Neurosci, **17** : 5-21, 2016.

13. Zhang Y, Wu KM, Yang L, *et al.* Tauopathies : new perspectives and challenges. Mol Neurodegeneration, **17** : 28, 2022.

14. Shoghi-Jadid K, Small GW, Agdeppa ED, *et al.* Localization of neurofibrillary tangles and beta-amyloid plaques in the brains of living patients with Alzheimer disease. Am J Geriatr Psychiatry, **10** : 24-35, 2002.

15. Maruyama M, Shimada H, Suhara T, *et al.* Imaging of tau pathology in a tauopathy mouse model and in Alzheimer patients compared to normal controls. Neuron, **79** : 1094-1108, 2013.

16. Hashimoto H, Kawamura K, Takei M, *et al.* Identification of a major radiometabolite of [^{11}C] PBB3. Nucl Med Biol, **42** : 905-910, 2015.

17. Okamura N, Furumoto S, Harada R, *et al.* Novel ^{18}F-labeled arylquinoline derivatives for noninvasive imaging of tau pathology in Alzheimer disease. J Nucl Med, **54** : 1420-1427, 2013.

18. Harada R, Okamura N, Furumoto S, *et al.* ^{18}F-THK5351 : A Novel PET Radiotracer for Imaging Neurofibrillary Pathology in Alzheimer Disease. J Nucl Med, **57** : 208-214, 2016.

19. Ng KP, Pascoal TA, Mathotaarachchi S, *et al.* Monoamine oxidase B inhibitor, selegiline, reduces ^{18}F-THK5351 uptake in the human brain. Alzheimers Res Ther, **9** : 25, 2017.

20. Marquié M, Normandin MD, Vanderburg CR, *et al.* Validating novel tau positron emission tomography tracer [F-18]-AV-1451 (T807) on postmortem brain tissue. Ann Neurol, **78** : 787-800, 2015.

21. Mattay VS, Fotenos AF, Ganley CJ, Marzella L. Brain tau Imaging : Food and Drug Administration approval of ^{18}F-Flortaucipir Injection. J Nucl Med, **61** : 1411-1412, 2020.

22. Jie CVML, Treyer V, Schibli R, Mu L. Tauvid™ : The first FDA-approved PET tracer for imaging tau pathology in Alzheimer's disease. Pharmaceuticals (Basel), **14** : 110, 2021.

23. Sander K, Lashley T, Gami P, *et al.* Characterization of tau positron emission tomography tracer [^{18}F]AV-1451 binding to postmortem tissue in Alzheimer's disease, primary tauopathies, and other dementias. Alzheimers Dement, **12** : 1116-1124, 2016.

24. Lowe VJ, Curran G, Fang P, *et al.* An autoradiographic evaluation of AV-1451 Tau PET in dementia. Acta Neuropathol Commun, **4** : 58, 2016.

25. Marquié M, Verwer EE, Meltzer AC, *et al.* Lessons learned about [F-18]-AV-1451 off-target binding from an autopsy-confirmed Parkinson's case. Acta Neuropathol Commun, **5** : 75, 2017.

26. Lee CM, Jacobs HIL, Marquié M, *et al.* ^{18}F-Flortaucipir Binding in Choroid Plexus : Related to Race and Hippocampus Signal. J Alzheimers Dis, **62** : 1691-1702, 2018.

27. Ikonomovic MD, Uryu K, Abrahamson EE, *et al.* Alzheimer's pathology in human temporal cortex surgically excised after severe brain injury. Exp Neurol, **190** : 192-203, 2004.

28. Choi JY, Cho H, Ahn SJ, *et al.* Off-Target ^{18}F-AV-1451 Binding in the Basal Ganglia Correlates with Age-Related Iron Accumulation. J Nucl Med, **59** : 117-120, 2018.

29. Ikonomovic MD, Abrahamson EE, Price JC, Mathis CA, Klunk WE. [F-18]AV-1451 positron emission tomography retention in choroid plexus : More than "off-target" binding. Ann Neurol, **80** : 307-308, 2016.

30. Vermeiren C, Motte P, Viot D, Mairet-Coello G, *et al.* The tau positron-emission tomography tracer AV-1451 binds with similar affinities to tau fibrils and monoamine oxidases. Mov Disord, **33** : 273-281, 2018.

31. Hansen AK, Brooks DJ, Borghammer P. MAO-B Inhibitors do not block in vivo Flortaucipir([^{18}F]-AV-1451) binding. Mol Imaging Biol, **20** : 356-360, 2018.

32. Yap SY, Frias B, Wren MC, *et al.* Discriminatory ability of next-generation tau PET tracers for Alzheimer's disease. Brain, **144** : 2284-2290, 2021.

33. Honer M, Gobbi L, Knust H, *et al.* Preclinical Evaluation of ^{18}F-RO6958948, ^{11}C-RO6931643, and ^{11}C-RO6924963 as Novel PET Radiotracers for Imaging Tau Aggregates in Alzheimer Disease. J Nucl Med, **59** : 675-681, 2018.

34. Wong DF, Comley RA, Kuwabara H, *et al.* Characterization of 3 Novel Tau Radiopharmaceuticals, ^{11}C-RO-963, ^{11}C-RO-643, and ^{18}F-RO-948, in Healthy Controls and in Alzheimer Subjects. J Nucl Med, **59** : 1869-1876, 2018.

35. Kuwabara H, Comley RA, Borroni E, *et al.* Evaluation of ^{18}F-RO-948 PET for Quantitative Assessment of Tau Accumulation in the Human Brain. J Nucl Med, **59** : 1877-1884, 2018.

36. Sanabria Bohórquez S, Marik J, Ogasawara A, *et al.* [^{18}F]GTP1 (Genentech Tau Probe 1), a radioligand for detecting neurofibrillary tangle tau pathology in Alzheimer's disease. Eur J Nucl Med Mol Imaging, **46** : 2077-2089, 2019.

37. Blennow K, Chen C, Cicognola C, *et al.* Cerebrospinal fluid tau fragment correlates with tau PET : a candidate biomarker for tangle patholo-

gy. Brain, **143** : 650-660, 2020.

38. Kroth H, Oden F, Molette J, *et al.* Discovery and preclinical characterization of [¹⁸F]PI-2620, a next-generation tau PET tracer for the assessment of tau pathology in Alzheimer's disease and other tauopathies. Eur J Nucl Med Mol Imaging, **46** : 2178-2189, 2019.

39. Mormino EC, Toueg TN, Azevedo C, *et al.* Tau PET imaging with ¹⁸F-PI-2620 in aging and neurodegenerative diseases. Eur J Nucl Med Mol Imaging, **48** : 2233-2244, 2021.

40. Baker SL, Provost K, Thomas W, *et al.* Evaluation of [¹⁸F]-JNJ-64326067-AAA tau PET tracer in humans. J Cereb Blood Flow Metab, **41** : 3302-3313, 2021.

41. Tagai K, Ono M, Kubota M, *et al.* High-Contrast In Vivo Imaging of Tau Pathologies in Alzheimer's and Non-Alzheimer's Disease Tauopathies. Neuron, **109** : 42-58.e8, 2021.

42. Ishizuchi K, Takizawa T, Tezuka T, *et al.* A case of progressive supranuclear palsy with predominant cerebellar ataxia diagnosed by [¹⁸F]PM-PBB3 tau PET. J Neurol Sci, **425** : 117440, 2021.

43. Zhou Y, Li J, Nordberg A, Ågren H. Dissecting the binding profile of PET tracers to corticobasal degeneration tau fibrils. ACS Chem Neurosci, **12** : 3487-3496, 2021.

44. Mishra SK, Yamaguchi Y, Higuchi M, Sahara N. Pick's tau fibril shows multiple distinct PET probe binding sites : insights from computational modelling. Int J Mol Sci, **22** : 349, 2020.

45. Knight AC, Morrone CD, Varlow C, Yu WH, McQuade P, Vasdev N. Head-to-head comparison of tau-PET radioligands for imaging TDP-43 in postmortem ALS brain. Mol Imaging Biol, 2022 ; 10.1007/s11307-022-01779-1.

46. Perez-Soriano A, Arena JE, Dinelle K, *et al.* PBB3 imaging in Parkinsonian disorders : Evidence for binding to tau and other proteins. Mov Disord, **32** : 1016-1024, 2017.

47. Koga S, Ono M, Sahara N, Higuchi M, Dickson DW. Fluorescence and autoradiographic evaluation of tau PET ligand PBB3 to α-synuclein pathology. Mov Disord, **32** : 884-892, 2017.

48. Walji AM, Hostetler ED, Selnick H, *et al.* Discovery of 6-(Fluoro-(¹⁸)F)-3-(1H-pyrrolo[2,3-c]pyridin-1-yl)isoquinolin-5-amine ([(¹⁸)F]-MK-6240) : A Positron Emission Tomography (PET) Imaging Agent for Quantification of Neurofibrillary Tangles (NFTs). J Med Chem, **59** : 4778-4789, 2016.

49. Leuzy A, Pascoal TA, Strandberg O, *et al.* A multicenter comparison of [¹⁸F]flortaucipir, [¹⁸F]RO948, and [¹⁸F]MK6240 tau PET tracers to detect a common target ROI for differential diagnosis. Eur J Nucl Med Mol Imaging, **48** : 2295-2305,

2021.

50. Hostetler ED, Walji AM, Zeng Z, *et al.* Preclinical characterization of ¹⁸F-MK-6240, a promising PET tracer for In vivo quantification of human neurofibrillary tangles. J Nucl Med, **57** : 1599-1606, 2016.

51. Pascoal TA, Shin M, Kang MS, *et al.* In vivo quantification of neurofibrillary tangles with [¹⁸F]MK-6240. Alzheimers Res Ther, **10** : 74, 2018.

52. Betthauser TJ, Cody KA, Zammit MD, *et al.* In vivo characterization and quantification of neurofibrillary tau PET radioligand 18F-MK-6240 in humans from Alzheimer disease dementia to young controls. J Nucl Med, **60** : 93-99, 2019.

53. Lohith TG, Bennacef I, Vandenberghe R, *et al.* Brain imaging of Alzheimer dementia patients and elderly controls with ¹⁸F-MK-6240, a PET tracer targeting neurofibrillary tangles. J Nucl Med, **60** : 107-114, 2019.

54. Pascoal TA, Therriault J, Benedet AL, *et al.* ¹⁸F-MK-6240 PET for early and late detection of neurofibrillary tangles. Brain, **143** : 2818-2830, 2020.

55. Aguero C, Dhaynaut M, Normandin MD, *et al.* Autoradiography validation of novel tau PET tracer [F-18]-MK-6240 on human postmortem brain tissue. Acta Neuropathol Commun, **7** : 37, 2019.

56. Salinas C, Lohith TG, Purohit A, *et al.* Test-retest characteristic of [¹⁸F]MK-6240 quantitative outcomes in cognitively normal adults and subjects with Alzheimer's disease. J Cereb Blood Flow Metab, **40** : 2179-2187, 2020.

57. Braak H, Braak E. Neuropathological stageing of Alzheimer-related changes. Acta Neuropathol, **82** : 239-259, 1991.

58. Braak H, Alafuzoff I, Arzberger T, Kretzschmar H, Del Tredici K. Staging of Alzheimer disease-associated neurofibrillary pathology using paraffin sections and immunocytochemistry. Acta Neuropathol, **112** : 389-404, 2006.

59. Gogola A, Minhas DS, Villemagne VL, *et al.* Direct Comparison of the Tau PET Tracers ¹⁸F-Flortaucipir and ¹⁸F-MK-6240 in Human Subjects. J Nucl Med, **63** : 108-116, 2022.

60. Shuping JL, Matthews DC, Adamczuk K, *et al.* Development, initial validation, and application of a visual read method for [¹⁸F]MK-6240 tau PET. Alzheimers Dement (NY). **9** : e12372, 2023.

61. Bennett RE, DeVos SL, Dujardin S, *et al.* Enhanced Tau Aggregation in the Presence of Amyloid β. Am J Pathol, **187** : 1601-1612, 2017.

62. Vogel JW, Iturria-Medina Y, Strandberg OT, *et al.* Spread of pathological tau proteins through communicating neurons in human Alzheimer's dis-

ease. Nat Commun, **11** : 2612, 2020.

63. Crary JF, Trojanowski JQ, Schneider JA, *et al*. Primary age-related tauopathy (PART) : a common pathology associated with human aging. Acta Neuropathol, **128** : 755-766, 2014.

64. Krishnadas N, Doré V, Groot C, *et al*. Mesial temporal tau in amyloid-β-negative cognitively normal older persons. Alzheimers Res Ther, **14** : 51, 2022.

65. Krishnadas N, Huang K, Schultz SA, *et al*. Visually Identified Tau ^{18}F-MK6240 PET Patterns in Symptomatic Alzheimer's Disease. J Alzheimers Dis, **88** : 1627-1637, 2022.

66. Villemagne VL, Doré V, Bourgeat P, *et al*. The Tau MeTeR composites for the generation of continuous and categorical measures of tau deposits in the brain. J Mol Med Ther, **1** : 25-32, 2017.

67. Harrison TM, Ward TJ, Murphy A, *et al*. Optimizing quantification of MK6240 tau PET in unimpaired older adults. Neuroimage, **265** : 119761, 2023.

68. Yamao T, Miwa K, Wagatsuma K, *et al*. Centiloid scale analysis for ^{18}F-THK5351 PET imaging in Alzheimer's disease. Physica medica, **82** : 249-254, 2021.

69. Mintun MA, Lo AC, Duggan Evans C, *et al*. Donanemab in Early Alzheimer's Disease. N Engl J Med, **384** : 1691-1704, 2021.

70. Rafii MS, Sperling RA, Donohue MC, *et al*. The AHEAD 3-45 Study : Design of a prevention trial for Alzheimer's disease. Alzheimers Dement, **19** : 1227-1233, 2023.